

PHOTOCHEMICAL PRODUCTION OF HYDROGEN FROM WATER*

EDMOND AMOUYAL and PHILIPPE KOFFI

*Laboratoire de Physico-Chimie des Rayonnements, Bâtiment 350, Université de Paris-Sud, 91405 Orsay (France)***Summary**

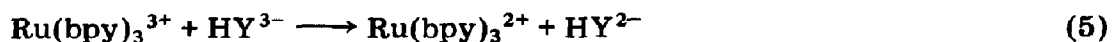
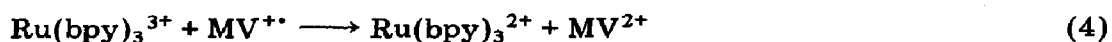
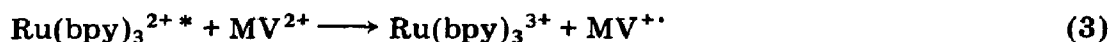
The quantum yields $\phi(\frac{1}{2}\text{H}_2)$ of hydrogen production were optimized as a function of the pH and the concentrations of the components of the $\text{Ru}(\text{bpy})_3^{2+}/\text{MV}^{2+}/\text{edta}/\text{colloidal platinum}$ model system ($\text{bpy} \equiv 2,2'$ -bipyridine; $\text{MV}^{2+} \equiv$ methylviologen; $\text{edta} \equiv$ ethylenediaminetetraacetic acid) irradiated at 453 nm. An optimum quantum yield $\phi(\frac{1}{2}\text{H}_2)$ of 0.171 ± 0.020 was found for the following optimized parameters: pH 5; $[\text{Ru}(\text{bpy})_3^{2+}] = 5.65 \times 10^{-5}$ M; $[\text{MV}^{2+}] = 3 \times 10^{-3}$ M; $[\text{edta}] = 0.1$ M; concentration of chemically prepared colloidal platinum, 1.92×10^{-5} M. The quantum yields of the methylviologen radical cation ($\text{MV}^{+\cdot}$) were determined under the same conditions, but without platinum, and an optimum value $\phi(\text{MV}^{+\cdot}) = 0.181 \pm 0.02$ was obtained. The hydrogen and $\text{MV}^{+\cdot}$ yields are thus closely related throughout the MV^{2+} concentration range investigated which supports the fact that colloidal platinum is operating with an efficiency close to 100%. Various types of heterogeneous catalysts (radiolytically prepared colloidal metals, metal deposited onto semiconductor powders, metal and metal oxide powders) were tested and compared under optimized experimental conditions. The relative catalytic efficiency of metal hydrosols for hydrogen production was as follows: iridium, platinum, osmium > ruthenium > rhodium > cobalt, nickel, palladium, silver, gold > copper, cadmium, lead. The highest $\phi(\frac{1}{2}\text{H}_2)$ was observed for colloidal iridium ($\phi(\frac{1}{2}\text{H}_2) = 0.173 \pm 0.020$). Pt-TiO₂ was found to be the most efficient of the supported metals ($\phi'(\frac{1}{2}\text{H}_2) = 0.160 \pm 0.020$). Hydrogen production from water was studied as a function of the nickel content (0.5 - 13.8 wt.%) for Ni-TiO₂ and an optimum yield $\phi'(\frac{1}{2}\text{H}_2) = 0.108 \pm 0.02$ was found for a nickel content of about 5 wt.%. RuO₂ and IrO₂ codeposited on zeolite gave the highest yields of the metal oxides ($\phi'(\frac{1}{2}\text{H}_2) = 0.102 \pm 0.02$). The efficiencies of low cost catalysts such as nickel powder, TiO₂, Fe₂O₃, Sm₂O₃, CeO₂, MnO₂ and ZnO were also examined.

*Paper presented at the Fifth International Conference on Photochemical Conversion and Storage of Solar Energy, Osaka, Japan, August 26 - 31, 1984.

1. Introduction

The photo-induced production of fuels from abundant materials as a means of solar energy storage is an expanding field in photochemistry. Among such studies, the photochemical generation of hydrogen and oxygen from water has received much attention and interest. Numerous model systems which are able to produce hydrogen and oxygen separately from water have been described [1]. These systems, which represent the reductive and oxidative components of the overall water-splitting reaction, are generally composed of a photosensitizer, an electron transfer relay, a sacrificial electron donor and an electron transfer catalyst. The first half-systems for the generation of hydrogen using visible light employed acridine yellow [2], proflavine [3] or $\text{Ru}(\text{bpy})_3^{2+}$ ($\text{bpy} \equiv 2,2'$ -bipyridine) [4 - 6] as photosensitizers, and PtO_2 [2, 6], K_2PtCl_6 [2, 4] or colloidal platinum [5] as catalysts. Oxygen has been photoproduced using a similar mechanism with RuO_2 as the catalyst [7, 8]. Complete splitting of water into hydrogen and oxygen has been reported [9] but it has not been possible to reproduce the results [10, 11].

The model system we have proposed comprises $\text{Ru}(\text{bpy})_3^{2+}$ as the photosensitizer, methylviologen (MV^{2+}) as the electron relay, the active form of ethylenediaminetetraacetic acid (edta) (HY^{3-}) as the donor and colloidal platinum as the catalyst [5, 12]. The reaction mechanism established from flash photolysis experiments [10, 12] is as follows:



For the first time it has been proved that colloidal dispersions of catalyst, used in a model system, mediate the production of hydrogen from water using visible light. In previous studies [4] the formation *in situ* of such

colloids had been assumed to occur through the reduction of platinum salts. We have also been able to establish that a metal oxide such as RuO_2 powder is an efficient catalyst for hydrogen production [13, 14]. The quantum yield $\phi(\frac{1}{2}\text{H}_2)$ of hydrogen formation has been found to be 0.087 [15] with colloidal platinum as the catalyst under the following experimental conditions: $\lambda_{\text{exc}} = 453 \text{ nm}$; pH 5; $[\text{Ru}(\text{bpy})_3^{2+}] = 5.65 \times 10^{-5} \text{ M}$; $[\text{MV}^{2+}] = 5 \times 10^{-4} \text{ M}$; $[\text{edta}] = 0.1 \text{ M}$; $[\text{Pt}] = 1.92 \times 10^{-5} \text{ M}$. It should be noted that several values of the hydrogen quantum yields have been reported but they are very scattered and range from 0.02 to 0.13 [10, 15 - 21] depending on the experimental conditions. It seems necessary to obtain a more precise characterization of this system which has been studied by various groups [18, 20 - 27] as a model for the photoconversion of solar energy. Therefore we have attempted to optimize the quantum yield of hydrogen formation as a function of the concentration of the various components of the system, *i.e.* $\text{Ru}(\text{bpy})_3^{2+}$, MV^{2+} , edta, colloidal platinum and H^+ . When these optimum conditions are defined, it will be possible to compare the efficiencies of various types of catalysts: colloidal metals, metals deposited onto semiconductor powders, and metal and metal oxide powders. This is the objective of the present study.

2. Experimental details

2.1. Materials

Two types of colloidal platinum sol were used in this study. The first was prepared according to the procedure of Rampino and Nord [28] and contained widely polydispersed particles [29]. The stabilizing polymer was poly(vinyl alcohol) (PVA) and the reducing agent was hydrogen. This chemically prepared colloidal platinum was used in all the $\phi(\frac{1}{2}\text{H}_2)$ optimization experiments. The second type of sol was prepared by the reduction of $\text{H}_2\text{PtCl}_6 \cdot 6\text{H}_2\text{O}$ induced by γ irradiation (^{60}Co source) and was stabilized with PVA [7]. The other colloidal metals were also radiolytically prepared (Table 1) in our laboratory using a method which is described in more detail elsewhere [30 - 33].

The origins of the metal and metal oxide powders are given in Table 2 and Table 3 respectively. The metal-supported catalysts were a gift from Dr. P. Pichat and Dr. J. M. Herrmann and were part of the same batch as those used in the work reported in refs. 34 - 36.

The sources of $\text{Ru}(\text{bpy})_3\text{Cl}_2$, MV^{2+} and edta have been specified previously [10].

2.2. Irradiation procedure

Argon-purged aqueous solutions (5 ml) buffered at the required pH (0.5 M) were irradiated at 453 nm using a xenon source (Osram XBO 2500 W) fitted to a 10 cm water filter and a Bausch and Lomb monochromator (10 nm bandwidth). The absolute photon flux $I_0 = 1.7 \times 10^{-7}$

TABLE 1

Quantum yields for hydrogen formation from the irradiation ($\lambda_{exc} = 453 \text{ nm}$) of aqueous solutions (pH 5) containing $5.65 \times 10^{-5} \text{ M Ru}(\text{bpy})_3^{2+}$, $3 \times 10^{-3} \text{ M MV}^{2+}$, 0.1 M ethylenediaminetetraacetic acid and various colloidal metals

Experiment	Catalyst	Method of preparation	Preparation	Particle diameter (Å)	Metal concentration ^a (M)	$\phi(\frac{1}{2}\text{H}_2)$ ^b
1	Pt	Chemical [10]	K ₂ PtCl ₄ -PVA	16 - 1000 [29]	1.92×10^{-5}	0.171
2	Pt ^c	Chemical [10]	K ₂ PtCl ₄ -PVA	16 - 1000 [29]	1.92×10^{-5}	0.105
3	Pt	Radiolytic [30]	K ₂ PtCl ₄ -PVA	15 [30]	2×10^{-5}	0.170
4	Pt ^d	Radiolytic [30]	K ₂ PtCl ₄	—	2×10^{-5}	0.100
5	Ir	Radiolytic [31]	H ₂ IrCl ₆ -PVA	12 [32]	2×10^{-5}	0.173
6	Ir	Radiolytic [31]	H ₂ IrCl ₆ -PVA	40 [32]	2×10^{-5}	0.173
7	Ir	Radiolytic [31]	H ₂ IrCl ₆ -PVA	<8 [32]	2×10^{-5}	0
8	Os	Radiolytic [33]	OsCl ₃ -PVA	— ^e	5×10^{-5}	0.160
9	Ru	Radiolytic [33]	RuCl ₅ -PVA	— ^e	6×10^{-5}	0.139
10	Rh	Radiolytic [33]	RhCl ₃ -PVA	— ^e	4×10^{-5}	0.080
11	Co	Radiolytic [33]	CoSO ₄ -PVA	— ^e	2×10^{-5}	0.066
12	Ni	Radiolytic [33]	NiSO ₄ -PVA	— ^e	4×10^{-5}	0.060
13	Pd	Radiolytic [33]	PdCl ₂ -PVA	— ^e	5×10^{-4}	0.056
14	Ag	Radiolytic [33]	AgNO ₃ -PVA	— ^e	2×10^{-5}	0.050
15	Au	Radiolytic [33]	HAuCl ₄ -PVA	— ^e	10^{-4}	0.042
16	Cu	Radiolytic [33]	CuSO ₄ -PVA	— ^e	$10^{-5} - 10^{-3}$	0
17	Cd	Radiolytic [33]	CdSO ₄ -PVA	— ^e	$10^{-5} - 10^{-3}$	0
18	Pb	Radiolytic [33]	PbClO ₄ -PVA	— ^e	$10^{-5} - 10^{-3}$	0

^aAs it is difficult to determine the concentration of the reduced metal precisely, the given optimum concentration can be considered as an approximation.

^bCorrected for light scattering effects by the colloidal particles.

^cNon-deaerated solution.

^dWithout PVA.

^eSols which do not precipitate and do not give the Tyndall effect (particle size, less than 50 Å).

TABLE 2

$\phi'(\frac{1}{2}\text{H}_2)^a$ for metal and metal-supported powders (same experimental conditions as Table 1)

Experiment	Catalyst	Origin	Metal loading (wt.%)	Particle diameter (Å)	Amount of catalyst added (mg)	$\phi'(\frac{1}{2}\text{H}_2)^a$
20	Co	Ugine carbone	—	—	14	0.060
21	Ni	Merck	—	—	16	0.110
22	Raney Ni	Merck	—	—	2	0.036
23	Pt black	Aldrich	—	—	14	0.058
24	Pt-Fe ₂ O ₃	[35]	0.5	—	12	Decomposes
25	Pt-SiO ₂	[35]	6.4	20	12	0.074
26	Pt-Al ₂ O ₃	[35]	0.6	30 - 35	12	0.120
27	Pt-TiO ₂	[34]	0.05	20 - 25	12	0.073
28	Pt-TiO ₂	[34]	0.5	20	12	0.160
29	Pt-TiO ₂	[34]	5	20 - 25	12	0.084
30	Pt-TiO ₂ ^b	[34]	5	20 - 25	12	0.160
31	Ni-TiO ₂	[36]	0.5	183	8	0.056
32	Ni-TiO ₂	[36]	4.83	135	8	0.108
33	Ni-TiO ₂	[36]	13.8	150	8	0.051
34	Ni-TiO ₂ ^b	[36]	13.8	150	8	0.104

^a $\phi'(\frac{1}{2}\text{H}_2)$ is $\phi(\frac{1}{2}\text{H}_2)$ uncorrected for light-scattering effects. It corresponds to a lower limit of $\phi(\frac{1}{2}\text{H}_2)$.

^bIn the presence of 2×10^{-3} M glutathione (Merck).

TABLE 3

$\phi'(\frac{1}{2}\text{H}_2)$ for metal oxide powders (same experimental conditions as Table 1)

Experiment	Catalyst	Origin	Amount of catalyst added (mg)	$\phi'(\frac{1}{2}\text{H}_2)$
40	RuO ₂ ·xH ₂ O	Alfa-Ventron	3	0.084
41	RuO ₂ -TiO ₂	[14]	5	0.087
42	RuO ₂ + IrO ₂ -zeolite	[14]	12	0.102
43	PtO ₂ ·xH ₂ O	Merck	22	0.072
44	TiO ₂	Degussa P 25	12	0.086
45	Fe ₂ O ₃	Prolabo	4	0.056
46	MnO ₂	Merck	3	0.042
47	WO ₃	Merck	6	0.039
48	Sm ₂ O ₃	Fluka	9	0.026
49	Nb ₂ O ₅	Fluka	6	0.026
50	ZnO	Prolabo	2	0.024
51	CeO ₂	Johnson-Matthey	4	0.018

einsteins s^{-1} was measured using a ferrioxalate actinometer [37]. The solutions were stirred in a cylindrical cell during irradiation to avoid concentration gradients.

2.3. Quantum yield determination

In order to measure the amount of hydrogen evolved, the irradiation cell was connected to a gas volumeter with a 2 ml scale [38]. The quantum yields of hydrogen production, obtained from the initial hydrogen formation rates, were corrected for light scattering by the catalyst particles unless otherwise stated.

The quantum yields for MV^{+} formation were measured in separate experiments in the absence of a catalyst. In this case aqueous solutions of $Ru(bpy)_3^{2+}$ (5.65×10^{-5} M), edta (10^{-1} M) and MV^{2+} (variable concentration) were deaerated by successive freeze-pump-thaw cycles. To determine the rate of formation of MV^{+} the growth of the 602 nm absorption band of the radical cation ($\epsilon_{MV^{+}} = 11\,000 \pm 1000$ $M^{-1} cm^{-1}$ [39]) was followed as a function of the irradiation time using a Beckman Acta MIV spectrophotometer.

3. Results and discussion

3.1. Optimization of the quantum yield of hydrogen generation

In a previous study [15] of the $Ru(bpy)_3^{2+}/MV^{2+}/edta$ /colloidal platinum system we established that there was no light intensity effect in the range investigated ($(2.9 - 24.9) \times 10^{-8}$ einsteins s^{-1}). In the present study the light intensity was kept constant ($I_0 = 1.7 \times 10^{-7}$ einsteins s^{-1}). Consequently, to optimize $\phi(\frac{1}{2}H_2)$ we examined the concentration effects of the various components of the system.

3.1.1. pH effect

We have shown previously [5, 10] that the rate of hydrogen production and the volume of hydrogen produced were pH dependent and reached a maximum at pH 5. Other workers have confirmed this result [20 - 22, 26] or found a very similar optimum pH of 4.7 [40]. Figure 1 shows the effect of the pH on $\phi(\frac{1}{2}H_2)$ for constant concentrations of the components of the system. It should be noted that the observed maximum at pH 5 is not very pronounced in this case and that there is a slight decrease in $\phi(\frac{1}{2}H_2)$ around the maximum between pH 3 and pH 6 which is of the order of 20% in agreement with recently published results [26] on relative yields of hydrogen. The existence of an optimum pH for hydrogen generation is due to two opposite effects. At low pH water reduction is easier but the concentration of the active form of edta (HY^{3-}) ($pK = 6.16$ [41]) decreases and therefore the deprotonation of HY^{2-} (reaction (7)) is slowed down [12]. At $pH > 5$ the HY^{2-} deprotonation is rapid but the reduction of water is inhibited. The small decrease in the hydrogen evolution rates upon increasing the pH above

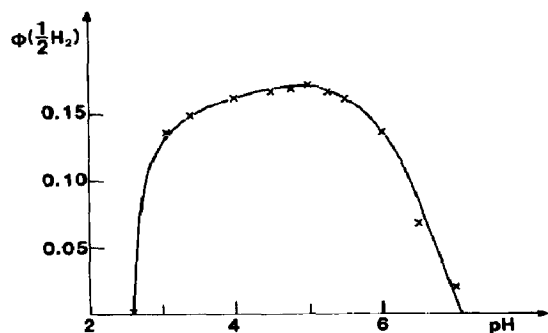


Fig. 1. Quantum yield of hydrogen formation vs. pH ($[Ru(bpy)_3^{2+}] = 5.65 \times 10^{-5}$ M; $[MV^{2+}] = 3 \times 10^{-3}$ M; $[edta] = 0.1$ M; $[Pt] = 1.92 \times 10^{-5}$ M). The quantum yields are corrected for light-scattering effects by the catalyst particles.

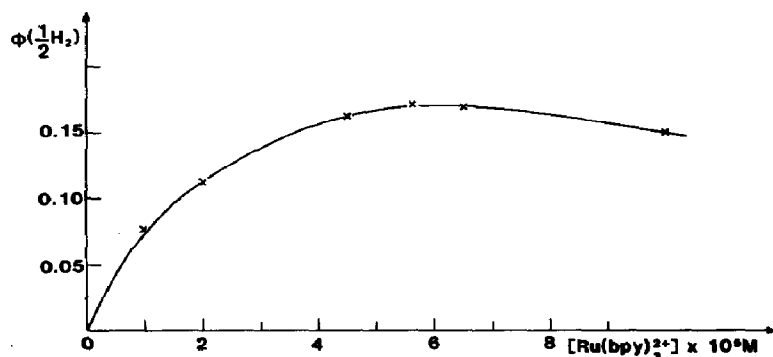


Fig. 2. Quantum yield of hydrogen formation vs. $Ru(bpy)_3^{2+}$ concentration ($[MV^{2+}] = 3 \times 10^{-3}$ M; $[edta] = 0.1$ M; $[Pt] = 1.92 \times 10^{-5}$ M; pH 5).

its optimum value has been attributed [26] to the selectivity of the colloidal platinum prepared radiolytically with respect to the MV^{2+} hydrogenation. However, further experiments are needed to confirm this explanation.

3.1.2. Effect of the concentration of $Ru(bpy)_3^{2+}$

The effect of the $Ru(bpy)_3^{2+}$ concentration on $\phi(\frac{1}{2}H_2)$ at pH 5 is shown in Fig. 2. $\phi(\frac{1}{2}H_2)$ increases with the $Ru(bpy)_3^{2+}$ concentration to a maximum value at 5.65×10^{-5} M and then decreases for higher concentrations. This classical behaviour corresponds to an inner-filter effect. Other perturbative effects (auto-absorption effect, excimer formation etc.) may be due to an excessively high concentration. The optimum $Ru(bpy)_3^{2+}$ concentration of 5.65×10^{-5} M was used in all subsequent experiments.

3.1.3. Effect of the ethylenediaminetetraacetic acid concentration

Figure 3 shows the effect of the edta concentration on $\phi(\frac{1}{2}H_2)$. The quantum yield of hydrogen increases with the edta concentration and reaches a plateau at concentrations above 2×10^{-2} M. A similar effect has been reported for the yield of the MV^{+} radical [42] and for the rate of

hydrogen production and volume of hydrogen produced [5, 10, 22]. Since edta is consumed during the reaction, a high constant edta concentration of 10^{-1} M has been used to ensure efficient $\text{Ru}(\text{bpy})_3^{3+}$ quenching (reaction (5)) and therefore to optimize $\phi(\frac{1}{2}\text{H}_2)$ and obtain large volumes of hydrogen.

3.1.4. Effect of methylviologen concentration

The effect of the MV^{2+} concentration on $\phi(\frac{1}{2}\text{H}_2)$ is shown in Fig. 4. This important effect has not been sufficiently emphasized. As for edta, saturation behaviour is observed with MV^{2+} . $\phi(\frac{1}{2}\text{H}_2)$ increases with increasing MV^{2+} concentration until a saturation concentration of 3×10^{-3} M is reached. This result agrees with the findings of an investigation of hydrogen formation rates as a function of the MV^{2+} concentration [22]. However, it should be noted that the hydrogen efficiencies determined here remain constant for MV^{2+} concentrations between 3×10^{-3} and 10^{-2} M.

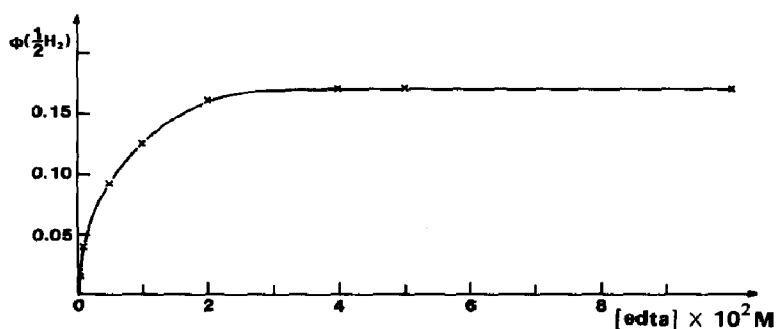


Fig. 3. Quantum yield of hydrogen formation vs. edta concentration ($[\text{Ru}(\text{bpy})_3^{2+}] = 5.65 \times 10^{-5}$ M; $[\text{MV}^{2+}] = 3 \times 10^{-3}$ M; $[\text{Pt}] = 1.92 \times 10^{-5}$ M; pH 5).

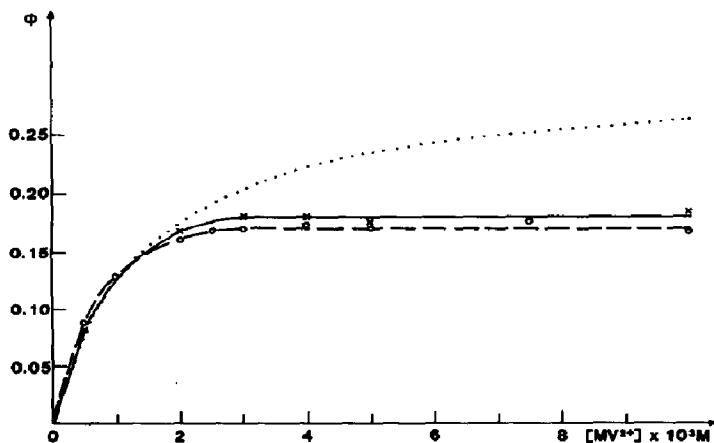


Fig. 4. Quantum yield of hydrogen formation vs. MV^{2+} concentration ($-\circ-$) ($[\text{Ru}(\text{bpy})_3^{2+}] = 5.65 \times 10^{-5}$ M; $[\text{edta}] = 0.1$ M; $[\text{Pt}] = 1.92 \times 10^{-5}$ M; pH 5); quantum yield of MV^{+} formation vs. MV^{2+} concentration ($-x-$) (same conditions as for previous curve but without colloidal platinum); calculated curve of $\phi(\text{MV}^{+})$ vs. MV^{2+} concentration according to eqns. (11) and (12) ($\phi_{ce} = 0.30$) (.....).

Reaction (9) shows that the hydrogen yield is related to the available $MV^{+•}$ radicals, and therefore to understand the effect of the MV^{2+} concentration on the hydrogen yield we have investigated its effect on the quantum yield $\phi(MV^{+•})$ of the $MV^{+•}$ radical cation. The $MV^{+•}$ yields were determined under the same experimental conditions as those used to determine $\phi(\frac{1}{2}H_2)$ but with no catalyst present ($\lambda_{exc} = 453$ nm; pH 5; $[Ru(bpy)_3^{2+}] = 5.65 \times 10^{-5}$ M; $[MV^{2+}] = 3 \times 10^{-3}$ M; $[edta] = 0.1$ M). It can clearly be seen in Fig. 4 that $\phi(MV^{+•})$ (full curve) and $\phi(\frac{1}{2}H_2)$ (broken curve) are very closely related. We obtained similar yields of $MV^{+•}$ and hydrogen for all the MV^{2+} concentrations investigated at the optimum platinum concentration (see Section 3.1.5). Consequently (i) the effect of the MV^{2+} concentration on $\phi(\frac{1}{2}H_2)$ is due mainly to the stationary concentration of $MV^{+•}$ and (ii) in our experiments the chemically prepared colloidal platinum catalyzes hydrogen production with an efficiency close to 100% for MV^{2+} concentrations up to 10^{-2} M. The result is the same as that previously obtained [15] for a single MV^{2+} concentration of 5×10^{-4} M, but has a value approximately half that found here for an MV^{2+} concentration of 3×10^{-3} M:

$$\phi(MV^{+•}) = 0.181 \pm 0.020$$

The quantum yield of $MV^{+•}$ is given by

$$\phi(MV^{+•}) = \phi_T \phi_q \phi_{ce} \quad (11)$$

where ϕ_T is the efficiency of quenching of the excited state of $Ru(bpy)_3^{2+}$ ($\phi_T = 1.0$), ϕ_q is the efficiency of quenching of $Ru(bpy)_3^{2+}$ by MV^{2+} and is given by

$$\phi_q = \frac{k_q [MV^{2+}]}{k_q [MV^{2+}] + k_0} \quad (12)$$

where k_0 and k_q are the rate constants of reaction (3) and reaction (2) respectively, and ϕ_{ce} is the cage escape yield which represents the efficiency of net formation of $Ru(bpy)_3^{3+}$ and $MV^{+•}$ from the solvent cage (ϕ_{ce} is 0.25 [19, 43] or 0.30 [6]).

If we use the values $k_q = 1.03 \times 10^9$ M⁻¹ s⁻¹ and $k_0 = 1.45 \times 10^6$ s⁻¹, which were determined by flash photolysis [10], we can calculate ϕ_q and hence $\phi(MV^{+•})$ for each MV^{2+} concentration. For $[MV^{2+}] \leq 2 \times 10^{-3}$ M the best fit with experiment is obtained for $\phi_{ce} = 0.30$. The result of the calculation is shown by the dotted curve in Fig. 4. The $MV^{+•}$ yields obtained using $\phi_{ce} = 0.25$ are slightly less than the experimental values. This could be the result of not taking into consideration in eqn. (11) the formation of $MV^{+•}$ via the reaction of MV^{2+} with the non-protonated form of edta (Y^{3-}) (reaction (8)). Y^{3-} coexists with the protonated form ($pK = 6.16$) at pH 5. Indeed, we have previously been able to demonstrate the existence of such a reaction at pH 7 [10]. For $[MV^{2+}] > 2 \times 10^{-3}$ M relation (11) does not take into account the observed plateau for $\phi(\frac{1}{2}H_2)$ (Fig. 4, broken curve) and its low value. We have no explanation to offer for this unexpected behaviour unless we admit that the equilibrium (reaction (9)) is shifted to the left at

high MV^{2+} concentrations. Thus more $MV^{+•}$ radicals are formed and the back reaction (reaction (4)) is favoured at the expense of the edta oxidation reaction (reaction (5)). In subsequent experiments we used an optimum MV^{2+} concentration of 3×10^{-3} M.

3.1.5. Effect of the colloidal platinum concentration

After our initial report of the effect of the platinum concentration on the rate of hydrogen production and the volume of hydrogen produced [10] and on $\phi(\frac{1}{2}H_2)$ [15], several groups [22, 26] studied its effect on relative hydrogen yields. The curve given by Harriman and Mills [22] exhibited a plateau for $[Pt] \geq 4 \times 10^{-7}$ M. However Rafaeloff *et al.* [26] have recently confirmed the existence of an optimum yield, but at a platinum concentration of 4.1×10^{-5} M.

Figure 5, which was obtained for the optimum experimental conditions established in this work (*i.e.* pH 5, $[Ru(bpy)_3^{2+}] = 5.65 \times 10^{-5}$ M, $[edta] = 0.1$ M and $[MV^{2+}] = 3 \times 10^{-3}$ M), shows behaviour similar to that initially observed [15] for non-optimized experimental conditions, in particular for an MV^{2+} concentration of 5×10^{-4} M. The quantum yield of hydrogen thus increases with increasing platinum content up to an optimum value

$$\phi(\frac{1}{2}H_2) = 0.171 \pm 0.020$$

which is reached at $[Pt] = 1.92 \times 10^{-5}$ M and then decreases at higher platinum concentrations. This value, which was determined under optimum experimental conditions, is close to the value $\phi(MV^{+•}) = 0.181 \pm 0.020$ found under the same conditions in the absence of platinum. The similarity between $\phi(\frac{1}{2}H_2)$ and $\phi(MV^{+•})$ is observed for $[Pt] \leq 2 \times 10^{-5}$ M. Therefore it should be emphasized that hydrogen is formed almost stoichiometrically (reaction (9)), which confirms [15] that the colloidal platinum operates with an efficiency close to 100% and explains the absence of any particle size influence on the platinum-mediated hydrogen evolution [15, 29].

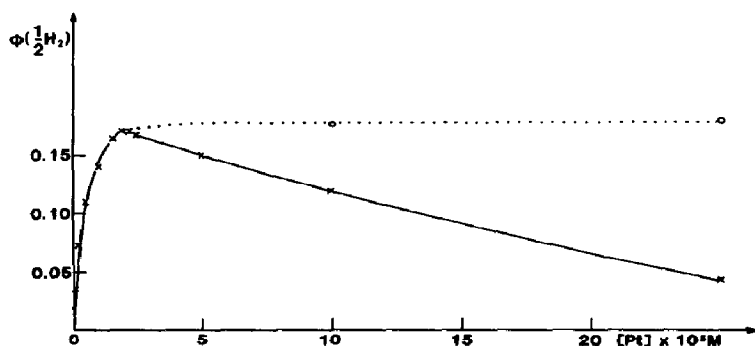


Fig. 5. Quantum yield of hydrogen formation *vs.* concentration of chemically prepared colloidal platinum: —x—, $[Ru(bpy)_3^{2+}] = 5.65 \times 10^{-5}$ M, $[MV^{2+}] = 3 \times 10^{-3}$ M, $[edta] = 0.1$ M, pH 5; ...o..., as for the previous curve but with the addition of 2×10^{-3} M glutathione.

We have attributed [15] the observed decrease in $\phi(\frac{1}{2}\text{H}_2)$ at platinum concentrations greater than 2×10^{-5} M to the MV^{2+} (MV^{2+}) hydrogenation reaction (reaction (10)) catalysed by colloidal platinum. The dotted curve in Fig. 5 shows that, if a hydrogenation catalyst poison such as glutathione [21] is used, $\phi(\frac{1}{2}\text{H}_2)$ increases and the values obtained are identical with the optimum hydrogen yield at all the platinum concentrations investigated. The resulting plateau thus demonstrates the existence of a $\phi(\text{MV}^{2+})$ optimum.

3.1.6. Concluding remarks on the optimization of $\phi(\frac{1}{2}\text{H}_2)$

Before concluding this discussion of the optimization of hydrogen quantum yields it should be emphasized that the effects of the concentrations of the various constituents are mutually independent. Indeed, if we vary one of the experimental conditions while keeping the other parameters constant, we obtain the same maximum for each constituent. This can be illustrated by the effect of the platinum concentration on $\phi(\frac{1}{2}\text{H}_2)$. The same optimum is observed for $[\text{Pt}] = 1.92 \times 10^{-5}$ M and for MV^{2+} concentrations varying between 5×10^{-4} [15] and 4×10^{-3} M, with the concentrations of $\text{Ru}(\text{bpy})_3^{2+}$ (5.65×10^{-5} M), edta (0.1 M) and H^+ (pH 5) kept constant. As a result the required experimental conditions to obtain optimum MV^{2+} yields (in the absence of a catalyst) and optimum hydrogen production (catalysed by chemically prepared colloidal platinum) are as follows: pH 5; $[\text{Ru}(\text{bpy})_3^{2+}] = 5.65 \times 10^{-5}$ M; $[\text{MV}^{2+}] = 3 \times 10^{-3}$ M; $[\text{edta}] = 0.1$ M; $[\text{Pt}] = 1.92 \times 10^{-5}$ M.

3.2. Comparison of various heterogeneous catalysts

It is necessary to develop highly active catalysts for hydrogen generation in order to achieve a complete photochemical water-splitting system. Having optimized the pH and the concentrations of $\text{Ru}(\text{bpy})_3^{2+}$, MV^{2+} and edta, we are now able to compare the efficiencies of various types of hydrogen production catalysts provided that their concentration is optimized in each case.

3.2.1. Colloidal metals

Since we first showed [5] that colloidal platinum and gold can mediate the photoreduction of water in a model system, the study of such catalysts for this purpose has developed considerably. These metal hydrosols can be prepared chemically or radiolytically. In this work we used colloidal platinum which was prepared chemically using the Rampino-Nord method [28] and compared it with various colloidal metals prepared radiolytically in our laboratory [30, 31, 33]. The radiolytic method, which was proposed in 1955 by Haissinsky and Pujol [44] and was developed by other researchers [26, 45, 46], has recently been optimized for catalysis purposes, and colloids of very small particle size (less than 50 Å (subcolloidal solutions)) have been obtained by Belloni and coworkers [30, 31, 33].

The results are given in Table 1. The group VIII metals, in particular the platinides (platinum, iridium and osmium), are extremely efficient catalysts of hydrogen production in the $\text{Ru}(\text{bpy})_3^{2+}/\text{MV}^{2+}/\text{edta}/\text{catalyst}$ model system. It is well known that these metals have the lowest overpotential for hydrogen production in water electrolysis cells [47]. However, the catalytic efficiency of other metals cannot easily be correlated with their overpotentials.

The relative order of metal catalytic activity for hydrogen evolution is as follows: iridium, platinum, osmium > ruthenium > rhodium > cobalt, nickel, palladium, silver, gold > copper, cadmium, lead. The highest value of $\phi(\frac{1}{2}\text{H}_2)$ is obtained for iridium hydrosols:

$$\phi(\frac{1}{2}\text{H}_2) = 0.173 \pm 0.020$$

Unlike Rafaeloff *et al.* [26], we found that the catalytic efficiencies of osmium and ruthenium were similar to that of platinum and that palladium had a low activity. This could be a result of the sample preparation conditions.

As in the case of chemically prepared platinum, $\phi(\frac{1}{2}\text{H}_2)$ depends on the concentration: the optimum yields for radiolytically prepared platinum and iridium are obtained for the same metal concentration of 2×10^{-5} M (Table 1, experiments 1 and 5). An optimum concentration different from 2×10^{-5} M may mean that the reduction of the metal salt by γ irradiation is incomplete (it is indeed difficult to determine the concentration of the reduced metal precisely), but it could also indicate an effect specific to the nature of the metal.

Table 1 shows that radiolytically prepared platinum is just as efficient as chemically prepared platinum. Moreover, the efficiency remains the same even though the particle sizes are different (experiments 1 and 3). This result confirms [15, 29] the absence of particle size effects on platinum-catalysed hydrogen generation for a wide range of sizes. Iridium exhibits the same behaviour except for very small particles (of diameter below 8 Å (experiment 7)) in which case the hydrogen yield drops dramatically. This suggests that there is a minimum size for the catalytic generation of hydrogen. As expected, colloidal platinum is less efficient in the absence of PVA (experiment 4) and when it is used in non-deaerated solutions (experiment 2) but the yield is still high. From a practical point of view it is important to note that non-noble metals such as colloidal cobalt and nickel catalyse the reaction fairly efficiently but the evolution of hydrogen ceases within 1 h for the nickel catalyst. However, it seems that the definition of the preparation conditions for the colloid requires improvement.

3.2.2. Metal powders and supported metals

Few investigations of the catalytic activity of metal powders have been performed because in most cases they react with water to give hydrogen. Therefore we have studied group VIII metals which are not attacked by

water. The results are given in Table 2. Platinum black is less efficient than colloidal platinum and the difference becomes greater if the activity is referred to a unit mass of the catalyst. Nevertheless if platinum is supported on a metal oxide, in particular TiO_2 (Table 2, experiment 28), the catalytic activity approaches that of colloidal platinum for a similar platinum particle size (Table 1, experiment 3) and for an optimum platinum content of 0.5% corresponding to a platinum concentration of 6×10^{-5} M. In contrast with the literature data [23] Pt-TiO₂ was not found to be more efficient than Pt-PVA. It should be remembered, however, that the reaction parameters used in ref. 23 were not optimized and therefore it was difficult to compare different catalysts.

Although the platinum percentage varies, Table 2 seems to indicate that the support plays a role: the semiconductor TiO_2 gives better results than Al_2O_3 which in turn is more efficient than SiO_2 . Pt- Fe_2O_3 decomposes in aqueous solutions and hydrogen production stops very quickly. Even though the catalyst did not absorb the visible light ($\lambda_{\text{exc}} = 453$ nm) used in our experiments this effect, although less pronounced, can be compared with that observed by Pichat *et al.* [35] for the photocatalytic generation of hydrogen from liquid methanol under UV illumination at room temperature using catalysts from the same batches as those employed here. The effect in our experiments may also be due to the particle sizes and the metal contents.

The work of Mičić and Nenadović [48] on Ni-Cr₂O₃ has shown the possibility of using nickel as a catalyst for water photoreduction rather than Co-TiO₂ which was found to have a low efficiency [49]. The use of non-noble metals, which are much cheaper than precious metals, is economically worthwhile if the efficiency and the longevity of this type of catalyst can be improved. Table 2 shows that nickel powder is much more efficient than colloidal nickel. Furthermore the volume of hydrogen obtained is larger and the duration of hydrogen evolution is longer. Raney nickel, although more finely divided than nickel powder, is less efficient and behaves like colloidal nickel, *i.e.* hydrogen evolution stops within 1 h. If we use TiO_2 as a support, which leads to the best results for platinum, the efficiency referred to unit mass is superior. Table 2 shows that this efficiency depends on the nickel content and reaches a maximum of $\phi'(\frac{1}{2}\text{H}_2) = 0.108$ for a content of 4.83% and a particle size of about 150 Å for the three samples investigated. The existence of such an optimum has also been observed by Prahov *et al.* [36] for hydrogen production from aliphatic alcohols by UV illumination of Ni-TiO₂ powder (same batch as used here) and Pt-TiO₂ powder (optimum platinum content, 0.5%) and was attributed to electron transfer from the titania to the metal. In our case, where the supported metals are not irradiated, it is more likely that this optimum is related to the metal-catalysed MV^{2+} hydrogenation (reaction (10)). Indeed, we observed that in the presence of glutathione the hydrogen yield reached an optimum for a nickel content of 13.8% (Table 2, experiments 33 and 34) and a platinum content of 5% (Table 2, experiments 29 and 30).

3.2.3. Metal oxides

The results are presented in Table 3. As has been shown previously [13, 14], ruthenium oxides, which are known to be good catalysts of the production of oxygen from water, are also efficient catalysts of hydrogen evolution from water. Their advantage over the platinides is that they do not catalyse the hydrogenation of the electron relay. The best catalyst consists of RuO₂ and IrO₂ codeposited on zeolite:

$$\phi'(\frac{1}{2} \text{H}_2) = 0.102 \pm 0.020$$

This yield, which is not corrected for light scattering, is comparable with that obtained using colloidal platinum but the catalyst concentration is about two orders of magnitude greater.

PtO₂, which was used as the catalyst in the first model system for the photoreduction of water [2], leads to much lower yields (approximately 55% less than those obtained with colloidal platinum). It is worth noting that TiO₂ gives a better yield than RuO₂.

Table 3 also shows that appreciable yields can be obtained with several metal oxides, in particular Fe₂O₃, Sm₂O₃, CeO₂, MnO₂ and ZnO which are relatively cheap.

4. Conclusion

In the present work we have systematically investigated the optimization of the quantum yield as a function of the concentration of the various components of the Ru(bpy)₃²⁺/MV²⁺/edta/colloidal platinum/H₂O model system. The optimum yield is found to be $\phi(\frac{1}{2} \text{H}_2) = 0.171 \pm 0.020$ for the following optimum concentrations: [Ru(bpy)₃²⁺] = 5.65 × 10⁻⁵ M; [MV²⁺] = 3 × 10⁻³ M; [edta] = 0.1 M; [Pt] = 1.92 × 10⁻⁵ M; pH 5. The hydrogen production appears to be closely related to the concentration of the MV^{•+} radical over the whole MV²⁺ concentration range investigated. Therefore in this concentration range the chemically prepared colloidal platinum catalyses the hydrogen generation with an efficiency of almost 100%. The Ru(bpy)₃²⁺/MV²⁺/edta/colloidal platinum system is thus well characterized and can be used satisfactorily as a reference for water photo-reduction.

Having optimized the component concentrations, we tested the efficiency of various types of catalyst: colloidal metals, metal powders, metals deposited onto semiconductor powders and metal oxide powders. Finely dispersed solutions of subcolloidal metals prepared radiolytically [30, 31, 33] had efficiencies comparable with that obtained for chemically prepared colloidal platinum [10]. The highest yield ($\phi(\frac{1}{2} \text{H}_2) = 0.173 \pm 0.020$) was obtained for iridium hydrosols. The metal powders and supported metals provided interesting results; in particular, Pt-TiO₂ with a very low metal content (0.5%) was very effective as expected. It is worth noting that nickel powder is economically attractive, particularly when supported nickel is used

rather than the more expensive group VIII metals. Indeed, such catalysts can be prepared industrially and can be easily recovered at the end of the reaction. However, in order to minimize the undesired hydrogenation of the electron relay (reaction (10)) and therefore to increase the lifetime of the system it appears preferable to use ruthenium oxides. A high yield was found for RuO₂ and IrO₂ codeposited onto zeolite ($\phi'(\frac{1}{2}\text{H}_2) = 0.102 \pm 0.020$). Lower yields, although still worthy of attention, were obtained with other metal oxides, particularly TiO₂, Fe₂O₃, Sm₂O₃, CeO₂, MnO₂ and ZnO which are relatively cheap.

In conclusion, this work demonstrates that the availability of a large variety of catalysts, some of which are capable of producing hydrogen with a very high efficiency, means that we can now envisage the practical use of such sacrificial systems for solar energy storage. Other catalysts have an economically interesting cost-to-efficiency ratio. The catalysts which have been investigated here are certainly potential candidates for components of a complete water-splitting system and for many other types of process.

Acknowledgments

We thank Dr. J. Belloni and Dr. J. L. Marignier for the radiolytically prepared colloidal metals and for many helpful discussions. We also thank Dr. P. Pichat and Dr. J. M. Herrmann for providing the samples of metal-supported powders and Dr. A. Bernas for her interest in this work.

References

- 1 S. Claesson and B. Holmström (eds.), *Solar Energy — Photochemical Processes Available for Energy Conversion, Project Results NE 1982:14*, National Swedish Board for Energy Source Development, Uppsala, 1982.
- 2 B. V. Koriakin, T. S. Dzhabiev and A. E. Shilov, *Dokl. Akad. Nauk S.S.S.R.*, 233 (1977) 620.
- 3 A. I. Krasna, *Photochem. Photobiol.*, 29 (1979) 267.
- 4 J. M. Lehn and J. P. Sauvage, *Nouv. J. Chim.*, 1 (1977) 449.
- 5 A. Moradpour, E. Amouyal, P. Keller and H. Kagan, *Nouv. J. Chim.*, 2 (1978) 547.
- 6 K. Kalyanasundaram, J. Kiwi and M. Grätzel, *Helv. Chim. Acta*, 61 (1978) 2720.
- 7 J. M. Lehn, J. P. Sauvage and R. Ziessel, *Nouv. J. Chim.*, 3 (1979) 423.
- 8 J. Kiwi and M. Grätzel, *Angew. Chem., Int. Edn. Engl.*, 18 (1979) 624.
- 9 K. Kalyanasundaram and M. Grätzel, *Angew. Chem., Int. Edn. Engl.*, 18 (1979) 701.
- 10 P. Keller, A. Moradpour, E. Amouyal and H. Kagan, *Nouv. J. Chim.*, 4 (1980) 377.
- 11 A. Harriman, *J. Photochem.*, 25 (1984) 33.
- 12 E. Amouyal and B. Zidler, *Isr. J. Chem.*, 22 (1982) 117.
- 13 E. Amouyal, P. Keller and A. Moradpour, *J. Chem. Soc., Chem. Commun.*, (1980) 1019.
- 14 P. Keller, A. Moradpour and E. Amouyal, *J. Chem. Soc., Faraday Trans. I*, 78 (1982) 3331.
- 15 E. Amouyal, D. Grand, A. Moradpour and P. Keller, *Nouv. J. Chim.*, 6 (1982) 241.
- 16 D. Miller and G. McLendon, *Inorg. Chem.*, 20 (1981) 950.
- 17 A. J. Frank and K. L. Stevenson, *J. Chem. Soc., Chem. Commun.*, (1981) 593.

- 18 J. Kiwi and M. Grätzel, *J. Am. Chem. Soc.*, **101** (1979) 7214.
- 19 M. Maestri and D. Sandrini, *Nouv. J. Chim.*, **5** (1981) 637.
- 20 O. Johansen, A. Launikonis, J. W. Loder, A. W. H. Mau, W. H. F. Sasse, J. D. Swift and D. Wells, *Aust. J. Chem.*, **34** (1981) 981.
- 21 O. Johansen, A. Launikonis, J. W. Loder, A. W. H. Mau, W. H. F. Sasse, J. D. Swift and D. Wells, *Aust. J. Chem.*, **34** (1981) 2347.
- 22 A. Harriman and A. Mills, *J. Chem. Soc., Faraday Trans. II*, **77** (1981) 2111.
- 23 J. M. Lehn, J. P. Sauvage and R. Ziessel, *Nouv. J. Chim.*, **5** (1981) 291.
- 24 M. Gohn and N. Getoff, *Z. Naturforsch.*, **34a** (1979) 1135.
- 25 K. Mandal and M. Z. Hoffman, *J. Phys. Chem.*, **88** (1984) 185.
- 26 R. Rafaeloff, Y. Haruvy, J. Binenboym, G. Baruch and L. A. Rajbenbach, *J. Mol. Catal.*, **22** (1983) 219.
- 27 M. T. Nenadović, O. I. Mičić, T. Rajh and D. Savić, *J. Photochem.*, **21** (1983) 35.
- 28 L. D. Rampino and F. F. Nord, *J. Am. Chem. Soc.*, **63** (1941) 2745.
- 29 P. Keller and A. Moradpour, *J. Am. Chem. Soc.*, **102** (1980) 7193.
- 30 M. O. Delcourt, N. Kéghouche and J. Belloni, *Nouv. J. Chim.*, **7** (1983) 131.
- 31 J. Belloni, M. O. Delcourt and C. Leclere, *Nouv. J. Chim.*, **6** (1982) 507.
- 32 J. Belloni, personal communication, 1984.
- 33 J. Belloni, J. L. Marignier, M. O. Delcourt and M. Minana, *Fr. Patent 84.09196* (1984).
- 34 P. Pichat, M. N. Mozzanega, J. Disdier and J. M. Herrmann, *Nouv. J. Chim.*, **6** (1982) 559.
- 35 P. Pichat, J. M. Herrmann, J. Disdier, H. Courbon and M. N. Mozzanega, *Nouv. J. Chim.*, **5** (1981) 627.
- 36 L. T. Prahov, J. Disdier, J. M. Herrmann and P. Pichat, *Int. J. Hydrogen Energy*, **9** (1984) 397.
- 37 C. G. Hatchard and C. A. Parker, *Proc. R. Soc. London, Ser. A*, **235** (1956) 518.
- 38 D. D. Davis and K. L. Stevenson, *J. Chem. Educ.*, **54** (1977) 394.
- 39 P. A. Trudinger, *Anal. Biochem.*, **36** (1970) 222.
- 40 J. Kiwi, *Chem. Phys. Lett.*, **83** (1981) 594.
- 41 M. J. L. Tillotson and L. A. K. Staveley, *J. Chem. Soc.*, (1958) 3613.
- 42 K. Takuma, Y. Shuto and T. Matsuo, *Chem. Lett.*, (1978) 983.
- 43 S. F. Chan, M. Chou, C. Creutz, T. Matsubara and N. Sutin, *J. Am. Chem. Soc.*, **103** (1981) 369.
- 44 M. Haissinsky and A. M. Pujo, *C. R. Acad. Sci.*, **240** (1955) 2530.
S. Rashkov and A. M. Koulkes-Pujo, *J. Chim. Phys. Phys.-Chim. Biol.*, **65** (1968) 911.
- 45 J. Pukies, W. Roebke and A. Henglein, *Ber. Bunsenges. Phys. Chem.*, **72** (1968) 842.
A. Henglein, *J. Phys. Chem.*, **83** (1979) 2858.
- 46 D. Meisel, *J. Am. Chem. Soc.*, **101** (1979) 6133.
- 47 S. Srinivasan and F. J. Salzano, *Int. J. Hydrogen Energy*, **2** (1977) 53.
- 48 O. I. Mičić and M. T. Nenadović, *J. Chem. Soc., Faraday Trans. I*, **77** (1981) 919.
- 49 A. Mills and G. Porter, *J. Chem. Soc., Faraday Trans. I*, **78** (1982) 3659.